MATERIALS SCIENCE

DNA sequence–directed shape change of photopatterned hydrogels via high-degree swelling

Angelo Cangialosi,[1]* ChangKyu Yoon,[2]* Jiayu Liu,[3] Qi Huang,[1] Jingkai Guo,[3] Thao D. Nguyen,[2,3] David H. Gracias,[1,2]† Rebecca Schulman[1,4]†

Shape-changing hydrogels that can bend, twist, or actuate in response to external stimuli are critical to soft robots, programmable matter, and smart medicine. Shape change in hydrogels has been induced by global cues, including temperature, light, or pH. Here we demonstrate that specific DNA molecules can induce 100-fold volumetric hydrogel expansion by successive extension of cross-links. We photopattern up to centimeter-sized gels containing multiple domains that undergo different shape changes in response to different DNA sequences. Experiments and simulations suggest a simple design rule for controlled shape change. Because DNA molecules can be coupled to molecular sensors, amplifiers, and logic circuits, this strategy introduces the possibility of building soft devices that respond to diverse biochemical inputs and autonomously implement chemical control programs.

If one region of a material shrinks or swells in response to a chemical or physical stimulus, the material can change shape to minimize its overall free energy (*1*–*4*). The ability to addressably deform different material regions can thus allow a material to take on many shapes. This principle has been used to create metamorphic materials (*5*) or soft robots (*6*) in which embedded wires direct local mechanical deformations (*5*–*7*). However, wires add bulk and require batteries or tethering. In contrast, chemomechanically responsive materials swell or shrink in response to chemical rather than electrical or pneumatic signals. Chemicals can diffuse over large distances and into small or tortuous spaces, and the huge number of chemicals that can be synthesized offers unprecedented tunability and specificity. Chemomechanical devices require no batteries and can easily be miniaturized and integrated with other devices.

Stimuli such as temperature, light, electromagnetic stimuli, or pH have commonly been used to direct shape change (*1*–*4*). These nonspecific stimuli can induce chemical or conformational changes throughout a material, leading to substantial swelling or shrinking. However, this lack of specificity also means that these stimuli cannot produce addressable control comparable to that in wired systems. We sought to determine whether we could build a combinatorial library of biomolecules, such as DNA sequences, where each species would direct the swelling of a specific material domain.

[1]Department of Chemical and Biomolecular Engineering, Johns Hopkins University, Baltimore, MD 21218, USA. [2]Department of Materials Science and Engineering, Johns Hopkins University, Baltimore, MD 21218, USA. [3]Department of Mechanical Engineering, Johns Hopkins University, Baltimore, MD 21218, USA. [4]Department of Computer Science, Johns Hopkins University, Baltimore, MD 21218, USA.
*These authors contributed equally to this work. †Corresponding author. Email: rschulm3@jhu.edu (R.S.); dgracias@jhu.edu (D.H.G.)

We focused on hydrogels, cross-linked networks of polymers in water, where structural changes can cause extensive expansion or contraction of the material as a whole. To study biomolecular actuation, we considered DNA–cross-linked polyacrylamide hydrogels (Fig. 1A and fig. S1) (*8*). DNA hybridization exchange processes can direct the release of particles (*9*) or melt, form, or stiffen these gels (*10*–*12*). Hybridization exchange can also induce size or shape changes of DNA-linked nanostructures (*13*), thin films (*14*), and colloidal crystals (*15*–*17*). However, although the exchange of a DNA strand can cause DNA–cross-linked gels to swell by 10 to 15%, this amount is typically insufficient to change the shape of macroscale gel architectures (*18*, *19*) (fig. S2).

Hence, a critical challenge in making DNA-triggered shape-changing hydrogels was to substantially increase the degree of swelling. We postulated that swelling would increase if we lengthened cross-links successively using a DNA hybridization cascade in which multiple DNA molecules are inserted into a duplex (*20*, *21*) (Fig. 1, A and B). To test this theory, we designed DNA sequences (hereafter referred to as "system 1") consisting of hydrogel cross-links and corresponding hairpins (H1 and H2) for the cascade.

Another challenge to enable addressable control was to reproducibly fabricate well-defined, multimaterial DNA hydrogel shapes capable of arbitrary shape change in three dimensions. We thus developed a photolithography process to pattern DNA hydrogels into precisely defined architectures. Although numerous photolithographic processes for silicon-based devices exist, protocols for photopatterning DNA hydrogels are largely absent, and the patterning process presents distinctive challenges. The moduli of DNA–cross-linked hydrogels are orders of magnitude lower than those of silicon or even many polymers (fig. S3); additionally, these hydrogels tend to adhere strongly to untreated glass and photomasks. Further, the ultraviolet light typically used for photopolymerization can damage DNA. We developed a process in which an optimized amount of light exposure drives fabrication to reduce DNA damage. Further, we created a process where structure thickness is controlled by solid spacers sandwiched between glass slides and an AutoCAD-designed chrome mask with coatings and sacrificial layers that enable liftoff (Fig. 2A) (*22*). Structures with lengths and widths on the millimeter to centimeter scales and thicknesses from 15 to hundreds of micrometers with multiple domains could be patterned serially using mask alignment with registry to underlying layers (*22*). Multiple structures could be fabricated in parallel, and after fabrication, structures were stable in buffer at 4°C for at least 4 months (fig. S4).

We fabricated hydrogel squares (dimensions: 0.06 mm by 1 mm by 1 mm) that contained system 1 cross-links (*22*). In the presence of system 1 hairpins, the hydrogels expanded substantially, whereas the gels in buffer containing an alternate DNA sequence did not expand (Fig. 2, C and D). Scanning electron micrographs of fixed samples showed that multiscale pores formed during expansion (Fig. 2E). Expansion took place unabated at a roughly linear rate (fig. S5 and movie S1).

We thus asked whether hydrogels could reliably expand to a desired final size. We modified the sequences of the polymerizing hairpins to create "terminator hairpins" (Fig. 1C). By tuning the relative concentrations of polymerizing and terminator hairpins, we could induce swelling of gels to a well-defined final size (Fig. 2F and fig. S5). Inclusion of 2% terminator hairpins produced high-degree but well-controlled swelling and was used in the remainder of our studies (movie S2).

We also found that we could tune the swelling rate. Thinner films swelled slightly faster, but swelling rates do not appear to be limited by the diffusion of DNA hairpins (fig. S6). Increasing the length of one of the toeholds that initiated the hairpin insertion process from three to four or six base pairs sped up expansion more markedly (fig. S7), as did increasing the hairpin concentration (fig. S8).

By designing DNA sequences for three more systems of cross-links and hairpins, we could addressably swell multiple domains (table S1). Hydrogels with each cross-link type swelled extensively in response to their corresponding hairpins but not to others (figs. S9 and S10). Hairpins also accumulated only in gels with their corresponding cross-link sequences (fig. S11).

To investigate how to design the shape change of composite multidomain architectures, we characterized DNA sequence–driven curling of model bilayer beams (Fig. 3A and fig. S12). Although the beams curled only slightly in DNA-free buffer because of different rates of solvent uptake by *N,N′*-methylenebis(acrylamide) (BIS)–cross-linked and DNA–cross-linked gels (Fig. 3A and fig. S13), they curled much more tightly when subsequently exposed to their corresponding hairpins (Fig. 3A and fig. S14).

We applied finite element analysis to study bilayer curving caused by DNA-induced swelling (supplementary text). The stress response of the gel was assumed to be the sum of an elastic component for the entropic response of the polymer network and the solvent pressure acting on the network derived from the Flory-Huggins theory (*23*). We determined the final shape of a structure after DNA-driven swelling by changing the Flory-Huggins parameter in the DNA- and BIS–cross-linked gel layers to achieve the experimentally measured volumetric swelling ratios within the different layers (*22*) (Fig. 3A) and then solving for the displacement field in the bilayer.

To set the remaining model parameters, we conducted an unconfined compression test and thus measured the Young's modulus of a BIS–cross-linked gel as 2.2 kPa (fig. S15) (*22*), which corresponds to a shear modulus of 733 Pa, assuming mechanical incompressibility (supplementary text). We then used the finite element model to fit the shear modulus (229 Pa) of the DNA gel to obtain the curvature of the bilayer measured in experiments.

We found that the effects of varying DNA gel thickness, modulus, and the degree of swelling (Fig. 3B) can be described by a simple design rule for the curvature $K = C\eta + K_0$ of the bilayer, where η is the bilayer ratio (*24*) calculated by (supplementary text)

$$\eta = \frac{AB(1+B)\Delta\theta}{t_{BIS}\left(1+4AB+6AB^2+4AB^3+A^2B^4\right)} \quad (1)$$

where $A = E_{DNA}/E_{BIS}$ is the ratio of the Young's modulus (in pascals) of the DNA and BIS gels, $B = t_{DNA}/t_{BIS}$ is the ratio of the thickness (in millimeters) of the DNA and BIS gels, and $\Delta\theta$ is the difference in the volumetric swelling ratio between the DNA and BIS gels. The initial curvature $K_0 = 0.2\ mm^{-1}$ and proportionality constant $C = 0.21$ were obtained from a linear regression of our simulation results (Fig. 3B).

This design rule indicates that the curvature is more sensitive to the DNA gel swelling ratio ($\Delta\theta$), with which the curvature varied linearly, than to the shear modulus or thickness of the DNA gel layer. The high degree of swelling was thus essential for extensive shape change. Further, there is an optimum thickness of the DNA gel for which curvature is maximized (Fig. 3C). A DNA gel layer that is too thin cannot exert enough force to bend the bilayer, whereas a DNA gel layer that is too thick is negligibly affected by the BIS gel layer and undergoes uniform swelling rather than folding.

The parameter study predicts that the high degree of swelling of the DNA gel could cause millimeter- to centimeter-thick structures to bend. For example, an initially flat 10-mm-long–by–7.23-mm-thick bilayer with optimum DNA gel thickness and a maximum swelling ratio of 3.72 ± 0.11 should fold into a complete circle after sequence-specific DNA-triggered actuation.

We next explored how structures with multiple different DNA sequence–responsive hydrogels could change into different shapes in response to different hairpin inputs. We fabricated flowers in which two groups of petals responded to two different sequences (fig. S16 and Fig. 4A). In the presence of both sets of sequences, all of the petals folded (Fig. 4B). Each set alone caused its corresponding petals to fold, and petals could be folded in sequence through stepwise exposure (Fig. 4, C and D). We attribute the twisting of the petals to misalignment errors during photopatterning of the gel layers. We further fabricated hydrogel "crab" devices, in which the antennae, claws, and legs each curled in response to their respective sequences, either all at once or sequentially (Fig. 4, E to G, and fig. S17). The structures remained in their actuated states for at least 60 days (fig. S18).

Biological tissues demonstrate the versatility and functionality of shape change driven by

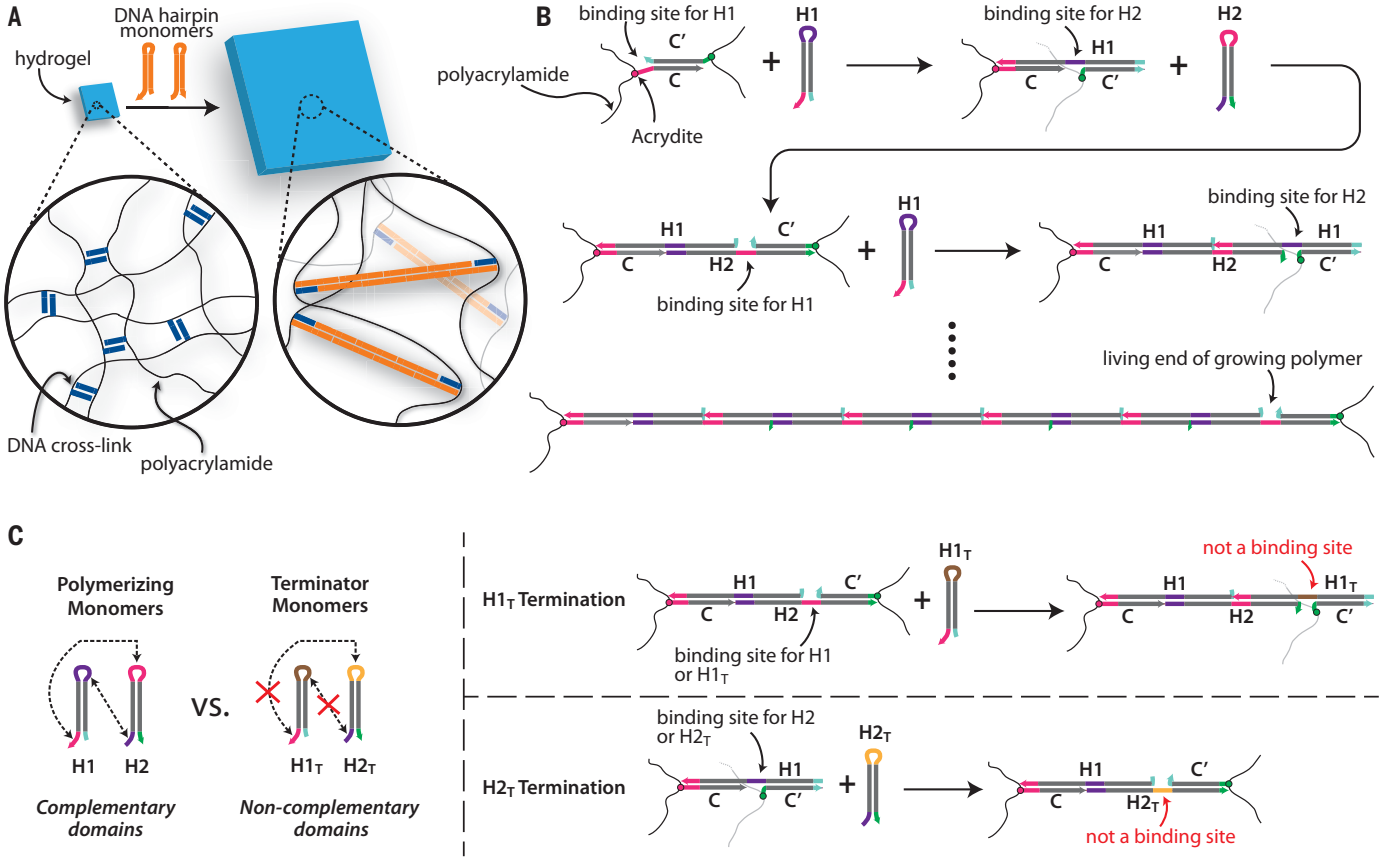

Fig. 1. DNA-directed expansion of DNA–cross-linked polyacrylamide gels. (**A**) DNA–cross-linked polyacrylamide hydrogels (*8*). Hairpins can insert into cross-links, inducing hydrogel expansion. (**B**) Schematic of cross-link C–C′ extension by hairpins H1 and H2. Colors indicate domain type and its complement. Thin black lines indicate polyacrylamide. (**C**) Polymerizing hairpins allow the insertion of additional monomers, whereas terminator hairpin monomers (denoted by "T") leave a site with which no monomers can interact.

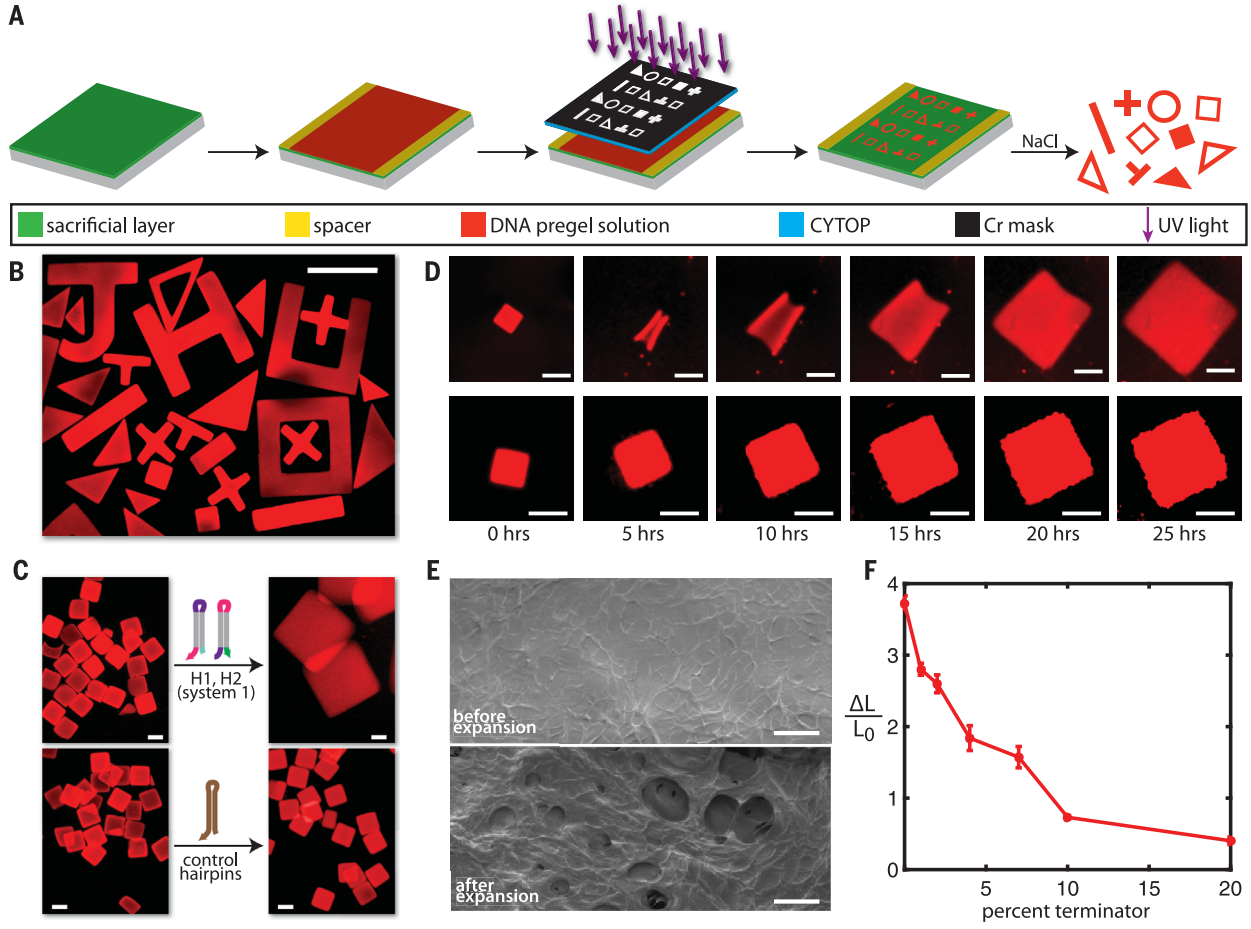

Fig. 2. Photopatterning and hydrogel expansion. (**A**) Photopatterning process flow. (**B**) Fluorescence micrograph of hydrogels poststained with SYBR Green I (*22*). Scale bar, 5 mm. (**C**) Hydrogels expand substantially in 20 μM polymerizing hairpin solution but not in 20 μM control hairpin solution. Scale bars, 1 mm. (**D**) Time-lapse fluorescence micrographs of a hydrogel in polymerizing hairpins (top) and 98% polymerizing, 2% terminating hairpins (bottom). Scale bars, 2 mm. (**E**) Scanning electron micrographs of hydrogels before and after DNA hybridization–driven expansion. Scale bars, 300 μm. (**F**) Linear expansion of hydrogels with different terminator hairpin percentages ($N = 4$ samples for each data point). Error bars represent 1 SD. L_0, initial length; ΔL, change in length.

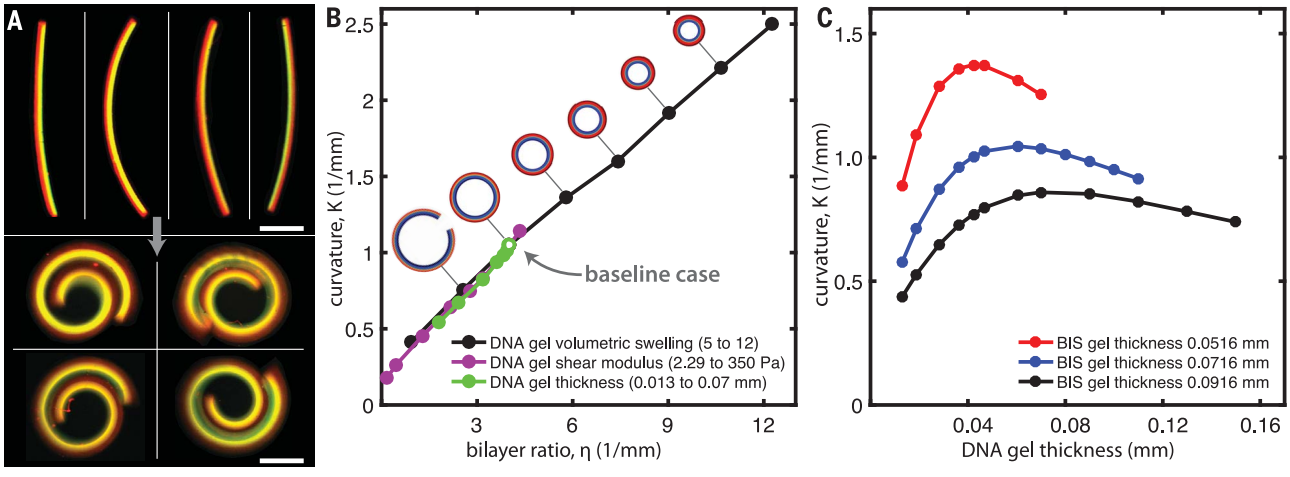

Fig. 3. Shape-change mechanics. (**A**) Fluorescence micrographs of photopatterned hydrogel beams (side views) with a 60-μm-thick BIS–cross-linked polyacrylamide layer (green) and a 60-μm-thick DNA–cross-linked hydrogel (red), before (top) and after (bottom) sequence-driven curving. Scale bars, 1 mm. (**B**) Computational finite element parameter study of bilayer curvature. The baseline case (white circle) corresponds to the experimentally measured bilayer curvature and swelling ratios. The bilayer ratio η (Eq. 1) captures the effects of the shear moduli, thickness, and volumetric swelling ratios of the gel layers. Illustrated bilayers show the predicted final shapes for different volumetric swelling ratios. (**C**) Analytical predictions of curvature change using the design rule $K = C\eta + K_0$, where C and K_0 were fit to the simulation results in (B).

biomolecules, where different cues and their concentrations determine which responses occur (*25*). We have demonstrated how specific biomolecular signals can also determine which domains of a synthetic material should change in shape and by how much. The DNA oligonucleotide signals used could be the outputs or inputs to molecular sensors (*26*) and circuits (*27*, *28*). Coupling these circuits to hydrogels could allow materials to exhibit multistage, goal-directed behaviors that are currently impossible to achieve (*4*, *29*, *30*). Because hairpin insertion and removal can occur while the cross-link remains connected (*20*), altering the extension reaction's bias could allow cross-link contraction and, potentially, reversible actuation. Finally, our wafer-scale patterning approach offers the potential for scale-up and integration with existing optical, logic, and memory devices.

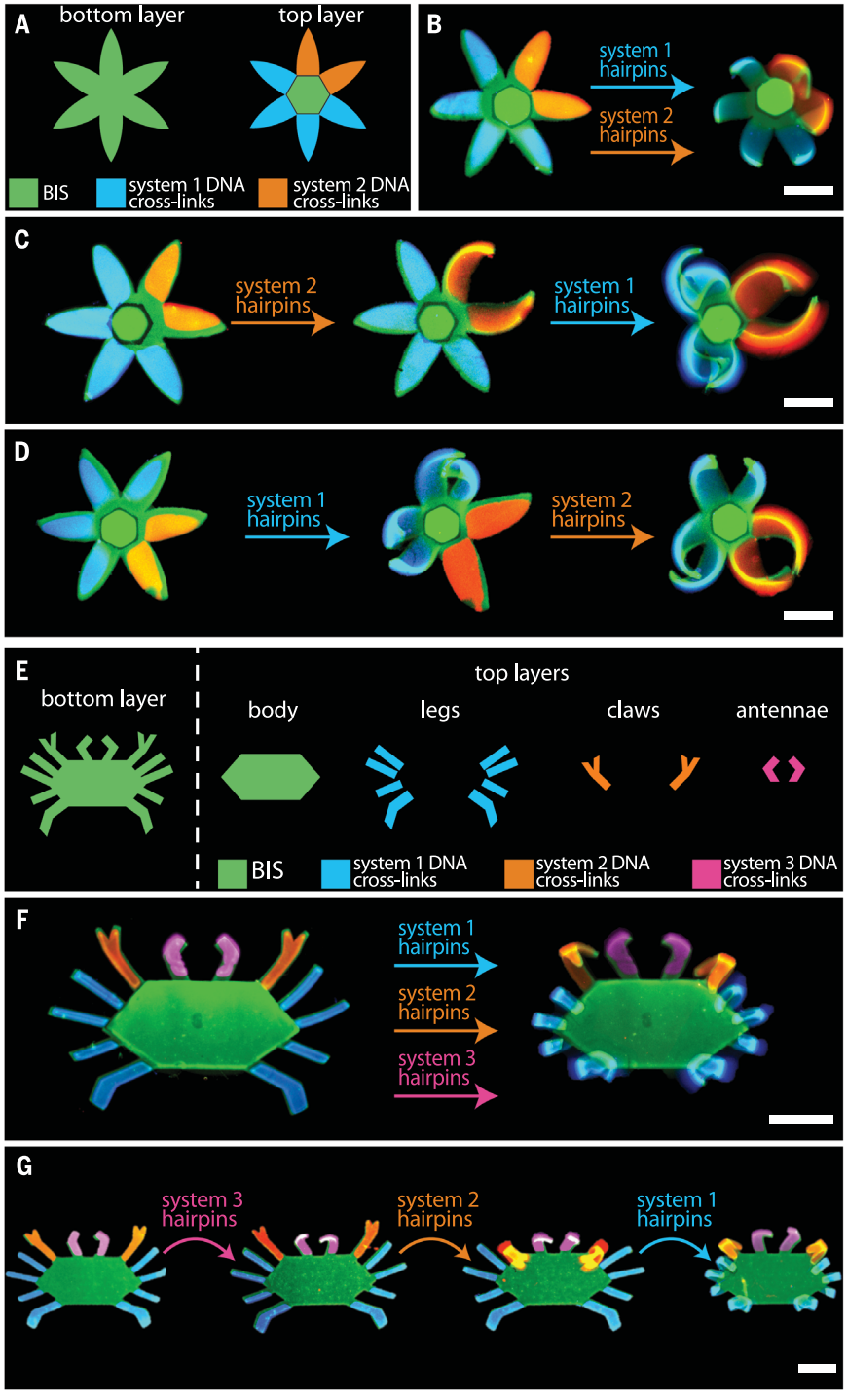

Fig. 4. DNA sequence–programmed shape change of macroscopic hydrogel shapes. (**A**) Schematic of a six-petal flower (*22*). (**B**) All petals curl in response to both system 1 and 2 hairpins. (**C** and **D**) Specific petals actuate in response to system 1 or system 2 hairpins alone. Petals can be actuated in series. (**E**) Hydrogel crab schematic. (**F**) Legs, claws, and antennae all actuate in response to system 1, 2, and 3 hairpins. (**G**) Serial actuation. Solutions contained 20 μM of each hairpin, 98% polymerizing hairpins, and 2% terminating hairpins. DNA–cross-linked hydrogel domains are differentially colored for clarity. Scale bars, 1 mm [(B) to (D)]; 2 mm [(F) and (G)].

REFERENCES AND NOTES

1. S. J. Jeon, A. W. Hauser, R. C. Hayward, *Acc. Chem. Res.* **50**, 161–169 (2017).
2. D. H. Gracias, *Curr. Opin. Chem. Eng.* **2**, 112–119 (2013).
3. Y. Liu, J. K. Boyles, J. Genzer, M. D. Dickey, *Soft Matter* **8**, 1764–1769 (2012).
4. L. D. Zarzar, J. Aizenberg, *Acc. Chem. Res.* **47**, 530–539 (2014).
5. D. Rus, M. T. Tolley, *Nature* **521**, 467–475 (2015).
6. F. Ilievski, A. D. Mazzeo, R. F. Shepherd, X. Chen, G. M. Whitesides, *Angew. Chem. Int. Ed.* **50**, 1890–1895 (2011).
7. E. Hawkes *et al.*, *Proc. Natl. Acad. Sci. U.S.A.* **107**, 12441–12445 (2010).
8. S. Nagahara, T. Matsuda, *Polym. Gels Netw.* **4**, 111–127 (1996).
9. T. Liedl, H. Dietz, B. Yurke, F. Simmel, *Small* **3**, 1688–1693 (2007).
10. Y. Hu *et al.*, *J. Am. Chem. Soc.* **138**, 16112–16119 (2016).
11. D. C. Lin, B. Yurke, N. A. Langrana, *J. Mater. Res.* **20**, 1456–1464 (2005).
12. J. S. Kahn, Y. Hu, I. Willner, *Acc. Chem. Res.* **50**, 680–690 (2017).
13. H. Yan, X. Zhang, Z. Shen, N. C. Seeman, *Nature* **415**, 62–65 (2002).
14. T. S. Shim *et al.*, *Nat. Nanotechnol.* **12**, 41–47 (2017).
15. Y. Kim, R. J. Macfarlane, M. R. Jones, C. A. Mirkin, *Science* **351**, 579–582 (2016).
16. Y. Zhang *et al.*, *Nat. Mater.* **14**, 840–847 (2015).
17. M. M. Maye, M. T. Kumara, D. Nykypanchuk, W. B. Sherman, O. Gang, *Nat. Nanotechnol.* **5**, 116–120 (2010).
18. Y. Murakami, M. Maeda, *Biomacromolecules* **6**, 2927–2929 (2005).
19. Y. Zhang, Y. P. Zhao, *J. Appl. Phys.* **99**, 053513 (2006).
20. S. Venkataraman, R. M. Dirks, P. W. K. Rothemund, E. Winfree, N. A. Pierce, *Nat. Nanotechnol.* **2**, 490–494 (2007).
21. F. Huang, X. Zhou, D. Yao, S. Xiao, H. Liang, *Small* **11**, 5800–5806 (2015).
22. Materials and methods are available as supplementary materials.
23. P. J. Flory, J. J. Rehner Jr., *J. Chem. Phys.* **11**, 512–520 (1943).
24. L. B. Freund, J. A. Floro, E. Chason, *Appl. Phys. Lett.* **74**, 1987–1989 (1999).
25. U. Alon, *An Introduction to Systems Biology* (CRC Press, 2006).
26. W. Zhou, P.-J. J. Huang, J. Ding, J. Liu, *Analyst* **139**, 2627–2640 (2014).
27. L. Qian, E. Winfree, *Science* **332**, 1196–1201 (2011).
28. D. Y. Zhang, G. Seelig, *Nat. Chem.* **3**, 103–113 (2011).
29. S. G. J. Postma, I. N. Vialshin, C. Y. Gerritsen, M. Bao, W. T. S. Huck, *Angew. Chem. Int. Ed.* **56**, 1794–1798 (2017).
30. M. Ikeda *et al.*, *Nat. Chem.* **6**, 511–518 (2014).

ACKNOWLEDGMENTS

We thank D. Scalise, J. Fern, J. Zenk, H. R. Kwag, A. M. Mohammed, D. Wirtz, and M. McCaffrey for discussions and technical assistance. We acknowledge funding from U.S. Army Research Office award W911NF-15-1-0490 and U.S. Department of Energy award 221874 for some materials characterization. All data are included in the article and supplementary materials. We declare no conflict of interest.

SUPPLEMENTARY MATERIALS

www.sciencemag.org/content/357/6356/1126/suppl/DC1
Materials and Methods
Supplementary Text
Figs. S1 to S20
Tables S1 and S2
References (*31*–*42*)
Movies S1 and S2

6 April 2017; accepted 16 August 2017
10.1126/science.aan3925

Science

DNA sequence–directed shape change of photopatterned hydrogels via high-degree swelling

Angelo Cangialosi, ChangKyu Yoon, Jiayu Liu, Qi Huang, Jingkai Guo, Thao D. Nguyen, David H. Gracias and Rebecca Schulman

Science **357** (6356), 1126-1130.
DOI: 10.1126/science.aan3925

Getting a hold with DNA

Stimuli-responsive materials can respond to physical or chemical cues to trigger changes in color, shape, or other properties. Cangialosi *et al.* used photolithography to define multilayer planar soft machines from polyacrylamide coupled to single strands of DNA. When presented with the complementary strands, the machines can change shape in complicated and programmable ways, including stepwise or sequential shape changes.

Science, this issue p. 1126